

Published in final edited form as:

J Endocrinol. 2009 October ; 203(1): 45–53. doi:10.1677/JOE-09-0068.

Functional Characterization of HCN Channels in Rat Pancreatic β Cells

Yi Zhang^{1,#,*}, Yunfeng Liu^{1,#}, Jihong Qu², Alexandre Hardy¹, Nina Zhang^{1,3}, Jingyu Diao¹, Paul J. Strijbos⁴, Robert Tsushima¹, Richard B. Robinson², Herbert Y. Gaisano¹, Qinghua Wang^{1,3,*}, and Michael B. Wheeler¹

¹Departments of Physiology and Medicine, University of Toronto, Ontario, Canada

²Department of Pharmacology, Columbia University, New York, U.S.A

³Division of Endocrinology and Metabolism, Li Ka-Shing Knowledge Institute, St Michael's Hospital, Toronto, Canada

⁴Neurology and GI Centre of Excellence for Drug Discovery, GlaxoSmithKline, New Frontiers Science Park, Harlow CM19 5AW, UK

Abstract

Hyperpolarization-activated cyclic nucleotide-gated (HCN) channels regulate pacemaker activity in some cardiac cells and neurons. In the present study, we have identified the presence of HCN channels in pancreatic β -cells. We then examined the functional characterization of these channels in β -cells via modulating HCN channel activity genetically and pharmacologically. Voltage-clamp experiments showed that over-expression of HCN2 in rat β -cells significantly increased HCN current (I_h), whereas expression of dominant-negative HCN2 (HCN2-AYA) completely suppressed endogenous I_h . Compared to control β -cells, over-expression of I_h increased insulin secretion at 2.8 mmol/l glucose. However, suppression of I_h did not affect insulin secretion at both 2.8 mmol/l and 11.1 mmol/l glucose. Current-clamp measurements revealed that HCN2 over-expression significantly reduced β -cell membrane input resistance (R_{in}), and resulted in a less hyperpolarizing membrane response to the currents injected into the cell. Conversely, dominant negative HCN2-AYA expression led to a substantial increase of R_{in} , which was associated with a more hyperpolarizing membrane response to the currents injected. Remarkably, under low extracellular potassium conditions (2.5mmol/l K^+), suppression of I_h resulted in increased membrane hyperpolarization and decreased insulin secretion. We conclude that I_h in β -cells possess the potential to modulate β -cell membrane potential and insulin secretion under hypokalemic conditions.

Keywords

pancreatic β -cell; HCN channels; insulin secretion; membrane potential; input resistance

INTRODUCTION

The current produced by hyperpolarization-activated cyclic nucleotide-gated (HCN) channels, termed I_h , has been recorded in a variety of cardiac cells and neurons. Unlike most voltage-

*Address correspondence to: Dr. Y Zhang, Departments of Physiology and Medicine, Room 7310, Medical Sciences Building, University of Toronto, 1 King's College Circle, Toronto, ON, Canada M5S 1A8 Tel: (416)-978-7160; Fax: (416)-978-8765; zany.zhang@utoronto.ca. Dr. Q Wang, St. Michael's Hospital, Room 7005, Queen Wing, 30 Bond Street, Toronto, ON., Canada M5B 1W8. Tel: (416) 864-6060 x6767; Fax: (416) 864-6043; qinghua.wang@utoronto.ca.

#These authors contributed equally to this work.

dependent channels, HCN channels are activated by membrane hyperpolarization and are permeable to both Na⁺ and K⁺ ions. To date, four mammalian HCN isoforms (HCN1-4) have been cloned. A major function of I_h is to serve as a pacemaker current in some excitable cells (Robinson & Siegelbaum 2003; DiFrancesco 1993). This pacemaker function is believed to play important roles in regulating heart rate and spontaneous electrical activity of neurons. In pyramidal neuron dendrites (Poolos *et al.* 2002), amacrine cells (Koizumi *et al.* 2004) and thalamocortical relay neurons (Meuth *et al.* 2006), I_h has been proposed to participate in controlling and stabilizing resting membrane potential. I_h has also been thought to be involved in the responses to sour taste, neuronal plasticity, and dendritic integration (reviewed in (Pape 1996; Robinson & Siegelbaum 2003; Wahl-Schott & Biel 2008)).

Pancreatic β-cells are electrically excitable cells that secrete insulin to maintain blood glucose homeostasis. A number of ion channels contribute to this function. Among these channels, the ATP-sensitive K⁺ (K_{ATP}) channel initiates membrane depolarization at high glucose and the voltage-dependent Ca²⁺ channel plays a key role for action potential firing and insulin secretion (Rorsman *et al.* 1994). We had reported that voltage-dependent K⁺ (K_v) channels are involved in the repolarization phase of the action potential; and that blockade of the K_v channel prolongs the action potential duration and enhances insulin secretion (MacDonald *et al.* 2002; MacDonald & Wheeler 2003). Recently, we demonstrated the presence of an HCN-encoded I_h in the pancreatic β-cell (El Kholy *et al.* 2007). In the present study, we further examine its functional characterization in regulation of electrical activity of pancreatic β-cells.

MATERIALS AND METHODS

Islet isolation and cell culture

Islets of Langerhans were isolated from male Wistar rats weighing 250–350g by collagenase digestion and separated by density gradient centrifugation, as described previously (MacDonald *et al.* 2001). Animal procedures were performed in accordance with the University of Toronto's Animal Care Committee's ethical guidelines. To obtain single islet cells, the intact rat islets were dispersed in dispase II solution (Roche, Germany) at 37°C for 5 min and the single cells were plated on glass coverslips. Intact islets or dispersed islet cells were cultured in RPMI 1640 medium containing 11.1 mmol/l glucose supplemented with 10% fetal bovine serum, 10 mmol/l HEPES, 100 units/ml penicillin, and 100 μg/ml streptomycin for 24–72 h before experiments.

Immunostaining and fluorescence confocal microscopy

Cells were fixed with 4% paraformaldehyde in PBS for 15 min and permeabilized with 0.2% Triton X-100 in PBS at room temperature for 10 min. Cells were then incubated with blocking solution containing 5% bovine serum albumin and 0.1% Triton X-100 in PBS at 37 °C for 30 min or 4°C for overnight. Subsequently, cells were co-incubated with anti-HCN (1:100, 1:100, 1:100 or 1:2000 for anti-HCN-1, HCN-2, HCN-3 or HCN-4, respectively) and anti-insulin (Dako, Denmark; 1:1000) primary antibodies for 16 h at 4°C. HCN antibodies were generated as previously described (Xiao *et al.* 2004). After washing, cells were stained with fluorescein-conjugated secondary antibodies. The coverslips were mounted with ProLong Gold antifade reagent (Invitrogen). Confocal laser scanning microscopy images analysis was performed using a Zeiss LSM-510 imaging system (Carl Zeiss, Oberkochen, Germany).

Adenoviral infection

We created an adenovirus expressing murine HCN2 (Ad-IRES-hrGFP-mHCN2) using the AdMax pdc516 shuttle vector (Microbix Biosystems, Toronto, Canada) as previously described (Qu *et al.* 2001), and incorporating green fluorescent protein (GFP) under the control of an IRES (Stratagene, La Jolla, CA). We similarly created the Ad-IRES-hrGFP-mHCN2-

AYA adenovirus, expressing a previously characterized (Er *et al.* 2003) dominant negative HCN2 construct in which the signature pore motif (GYG₄₀₂₋₄₀₄) of mHCN2 is mutated to AYA. For control experiments, an adenoviral GFP vector was used. Islet cells were transduced as previously described (Er *et al.* 2003; Qu *et al.* 2001). The multiplicity of infection (MOI; ratio of viral units to cells) was 100–150. The islets or cells were incubated in infection medium containing the adenoviruses for 2–3 hours at 37°C, after which the medium was replaced with culture medium and further cultured for 48–72 hours before experiments. Under these conditions, the infection efficiency was routinely 80–90% as determined by GFP expression.

Western blotting analysis

Expression of HCN2 proteins in rat islets adenovirally infected were determined by Western blot. Rat brain was used as a positive control. Cell lysates (25 µg) were subjected to SDS-PAGE and transferred to polyvinylidene difluoride-plus membranes (Fisher Scientific Ltd, Nepean, ON). Membranes were probed with the antibody for HCN2 (1:800 dilution). The bound primary antibody was detected with peroxidase-conjugated secondary anti-rabbit antibody (1:30000; Jackson ImmunoResearch Laboratories, West Grove, PA) and visualized by chemiluminescence (ECL-Plus, GE Healthcare, Mississauga, ON).

Electrophysiology

Cells were patch-clamped in perforated whole-cell configuration at 33–34°C. β-cells were identified by cell size (>4 pF) and their depolarization response to 11.1 mmol/l glucose (Manning Fox *et al.* 2006; Wendt *et al.* 2004). The measurements were performed using EPC-9 amplifier and PULSE software from HEKA Elektronik (Lambrecht, Germany). Patch pipettes were pulled from 1.5 mm thin-walled borosilicate glass tubes using a two-stage Narishige micropipette puller (Tokyo, Japan). The pipettes had typical resistances of 3–6 MΩ when fire polished and filled with an intracellular solution containing 140 mmol/l KCl; 1 mmol/l MgCl₂; 0.05 mmol/l EGTA; 10 mmol/l NaCl; 10 mmol/l HEPES; pH 7.3 adjusted with KOH. Gramicidin was added to the intracellular solution to a final concentration of 60 µg/ml immediately before the experiment. Standard extracellular solutions contained 138 mmol/l NaCl; 5.6 mmol/l KCl; 1.2 mmol/l MgCl₂; 2.6 mmol/l CaCl₂; 5 mmol/l HEPES; 11.1 mmol/l glucose; pH 7.4 adjusted with NaOH. For membrane potential recordings in figure 6, 2.8 mmol/l glucose was also used. For the low potassium extracellular solution used in figure 7, 138 mmol/l NaCl and 5.6 mmol/l KCl from standard extracellular solution were replaced by 140 mmol/l NaCl and 2.5 mmol/l KCl. All perforated patch recordings were achieved with serial resistance below 25 MΩ, and leak subtraction protocol was not applied. In current-clamp mode, membrane potential responses were measured from whole rat islets. The membrane input resistance (R_{in}) was estimated by Ohm's law $R_{in} = U/I$, where U is the membrane voltage measured at the end of current (I) injection. The equilibrium potential for potassium (E_K) was calculated by Nernst equation. ZD7288 was purchased from Tocris (Ellisville, MO).

Static Insulin Secretion Assay

After 72 hours post-infection, the islets (10/vial) were pre-incubated with glucose free Krebs-Ringer HEPES buffer (KRB, 125 mmol/l NaCl, 5.6 mmol/l KCl, 1.28 mmol/l CaCl₂, 5.0 mmol/l NaCO₃, 25 mmol/l HEPES, and 0.1% (w/v) bovine serum albumin) for 30 min, followed by incubation with 2.8 or 11.1 mmol/l glucose in KRB for 90-min. The supernatants of the islets were collected and centrifuged at 300 g × for 10 min to remove cell debris and insulin was measured by radioimmunoassay (Dai *et al.* 2006). The islets were then used for cell viability assessment. The insulin secretion data were normalized by the islet cell viability via an XTT absorbance assay. The XTT cell proliferation assay (Proliferation Kit II; Roche Applied Sciences, Laval, QC, Canada) was performed according to the manufacturer's instructions and as we have previously shown (Targonsky *et al.* 2006). Briefly, after insulin secretion

experiments, the islets were immediately incubated with the XTT reagent for 6 hours and the absorbance readings at 490 nm were recorded.

Islet perfusion secretory assay

After 72 hours post-infection, batches of 50 islets were placed in perfusion chambers with a capacity of 1.3 ml at 37°C and perfused with KRB at a flow rate of 1 ml/min as described above. For the low potassium extracellular solution used in figure 8, 128 mmol/l NaCl and 2.5 mmol/l KCl were used to replace the original concentrations of NaCl and KCl in the KRB. Islets were stimulated with 2.8 or 16.7 mmol/l glucose in the presence or absence of Forskolin (10 uM, Sigma-Aldrich Ltd., Oakville, Canada;) plus 3-isobutyl-1-methylxanthine (IBMX, 100 uM, Sigma-Aldrich Ltd) as indicated. Fractions were collected for insulin determination using a radioimmunoassay kit (Linco Research, St. Louis, MO). At the end of each perfusion, islets were collected and lysed in acid ethanol for assessment of insulin content. Results are presented as insulin secreted normalized to total insulin content.

Statistical analysis

All data are presented as means \pm SEM. Statistical analysis was done by Student's t test or paired t test and significance was assumed at a p value of less than 0.05. All calculations were made by SigmaPlot (SigmaPlot 2001, SPSS Science, USA). Patch clamp data were analysed with IGOR Pro3.12 software (Wavemetrics, Lake Oswego, OR).

RESULTS

HCN channels are expressed in rat β -cells

Four members of the HCN gene family (HCN1-4) are currently known (Ludwig *et al.* 1998; Santoro *et al.* 1997; Santoro *et al.* 1998). We therefore used specific antibodies of each of these HCN isoforms, which detected the presence of all four HCN isoforms in primary rat β -cells (Fig. 1). These results are consistent with our previously reported real-time PCR analysis of rat islet mRNA (El Kholy *et al.* 2007). Of note, some non- β -cells (see arrows pointing at non-insulin staining cells) are also positive for HCN, indicating that HCN channels are also expressed in other types of islet cells (Zhang *et al.* 2008).

Electrophysiological properties of native I_h in rat β -cells

We investigated the native I_h in rat β -cells. As shown in Figure 2A, hyperpolarizing voltages elicited slow activating inward currents (Fig. 2Aii), while application of HCN channel blocker, ZD7288 (50 uM), inhibited these currents (Fig. 2Aiii). On average, ZD7288 blocked $67.9 \pm 7.2\%$ ($p < 0.01$, $n=6$) of the sustained I_h obtained at -140 mV. Since both Na^+ and K^+ permeate HCN channels, the reversal potentials of I_h are between approximately -50 and -20 mV in many native pacemaker cell types (Accili *et al.* 2002; Pape 1996). To test the ion selectivity of I_h in rat β -cells, a current-voltage (I/V) relationship of the fully activated HCN channel was plotted and the reversal potential of I_h was obtained at -38 mV (Fig. 2Bii and 2Biii), suggesting that I_h in β -cells is a mixed cationic current of Na^+ and K^+ (Tian & Shipston 2000). These data clearly showed that native I_h in rat β -cells possesses typical properties of HCN channels as reported in other cell types (Kaupp & Seifert 2001; Ludwig *et al.* 1999; Yu *et al.* 2004).

Effects of over-expression or dominant-negative suppression of HCN channels on I_h

In order to investigate the functional role of I_h , we employed an adenoviral gene transfer strategy to manipulate HCN channel gene expression and current magnitude in primary β -cells (Qu *et al.* 2001). Cells transduced with GFP alone were used as control. Western blotting results show that the level of HCN2 proteins was effectively enhanced after infection (Fig 3A). Patch-clamp study demonstrates that over-expression of HCN2 in the islet β -cells resulted in a

significant increase in inward currents (Fig 3Biii) compared with GFP control (Fig 3Bi). Figure 3C illustrates the voltage-dependent I/V relationships of the HCN channel. The mean current density in HCN2-transduced cells was approximately sixteen-fold greater than that in control cells at -140 mV (66 ± 9 pA/pF for HCN2, $n=7$; 4.1 ± 0.5 pA/pF for GFP control, $n=6$; $p<0.001$); in contrast, expression of dominant-negative HCN2-AYA almost completely suppressed endogenous I_h (0.3 ± 0.3 pA/pF for HCN2-AYA, $n=7$; $p<0.001$ vs control, Fig 3Bii and C).

To determine the steady-state activation of these channels, tail currents induced by a -140 mV pulse were measured and the data were fit using the Boltzmann equation (Yagi & Sumino 1998). As shown in Figure 3D, the tail current amplitudes displayed typical sigmoidal properties (Ludwig *et al.* 1999). The half-maximal activation ($V_{1/2}$) voltage was -97 ± 1 mV in GFP control and -96 ± 1 mV in HCN2 group (Fig. 3D).

Influence of I_h on insulin secretion

Since ion channels play a pivotal role in regulation of insulin secretion, we next sought to determine whether insulin secretion is affected by HCN channel modulation. Our static insulin secretion data show HCN2-over-expression increased insulin secretion at 2.8 mmol/l glucose, but not change the secretion at 11.1 mmol/l glucose when compared with GFP control (Fig. 4A–B). No difference was observed for insulin secretion between HCN2-AYA-transduced and GFP-transduced islets at both glucose concentrations (Fig. 4A–B). To further confirm the results, we employed islet perfusion to investigate the effect of HCN channels on dynamic insulin secretion. We find HCN2-AYA did not change the insulin secretion pattern compared to GFP control even in the presence of forskolin/IBMX (Fig. 4C–D).

Influence of I_h on membrane input resistance (R_{in})

Membrane input resistance (R_{in}) is an important parameter of the intrinsic membrane properties, which determines membrane voltage responses to input currents (i.e. the currents flowing across the membrane). In general, the membrane voltage response is more sensitive to input current when R_{in} is high. It has been shown that I_h participates in regulation of R_{in} and thereby cell excitability in neurons (Magee 1998; Poolos *et al.* 2002; Poolos *et al.* 2006). To assess if I_h influences R_{in} in rat β -cells, we measured voltage responses to a set of injected hyperpolarizing currents under current-clamp mode. As shown in GFP-transduced cells, hyperpolarizing current produced a depolarizing voltage sag (or inflexion) (Fig 5Aii, indicated by dashed arrow); this voltage sag reflected the activation of I_h that depolarizes the membrane potential. Compared to GFP control, the hyperpolarizing current resulted in a more significant depolarizing sag in HCN2-transduced cells because of the enhanced I_h (Fig 5Aiii). Figure 5B shows that the mean R_{in} (calculated from -20 to -60 pA of injected currents) was lower in HCN2 (from 935 ± 115 M Ω to 548 ± 54 M Ω , $n=7$, $p<0.05$ vs control) than that in GFP control cells (from 1375 ± 159 to 998 ± 88 M Ω , $n=8$); in contrast, the mean R_{in} of HCN2-AYA ranged from 2179 ± 306 to $1540 + 100$ M Ω being substantially higher ($n=6$, $p<0.05$ vs control). Since I_h has been reported to limit membrane potential from increased hyperpolarization in neurons (Poolos *et al.* 2002), we thus tested if this occurs in rat β -cells. As seen (Figure 5Aii–Aiv), the difference between voltages induced by -20 and -140 pA injected currents ($\Delta V = V_{-20 \text{ pA}} - V_{-140 \text{ pA}}$) was calculated. We found HCN2 over-expression significantly decreased ΔV compared to GFP control (26 ± 4 mV for HCN2 over-expression, $n=7$; 67 ± 6 mV for GFP control, $n=6$; $p<0.001$, Fig. 5C), suggesting that I_h can prevent membrane potential from hyperpolarization in β -cells.

Influence of I_h on membrane hyperpolarization

We therefore next examined whether HCN channel modulation can affect the natural membrane potential responses. Membrane potential recordings from whole rat islets were

performed in standard extracellular solution containing 5.6 mmol/l KCl. Figure 6 shows membrane potential responses at 11.1 and 2.8 mmol/l glucose concentrations in GFP- (Fig. 6A) or HCN2-AYA-transduced islets (Fig. 6B). It is shown that dominant-negative HCN2-AYA did not cause significant change of the mean membrane potentials at low or high glucose concentrations compared with GFP control (-41 ± 3 mV at 11.1 mmol/l glucose and -61 ± 2 mV at 2.8 mmol/l glucose for HCN2-AYA, $n=5$; vs -41 ± 2 mV at 11.1 mmol/l glucose and -55 ± 4 mV at 2.8 mmol/l glucose for GFP control, $n=5$, $p>0.05$; Fig. 6C).

We then tested the membrane potential responses from non-adenovirus-infected islets in extracellular solution containing low potassium (2.5 mmol/l KCl) and 11.1 mmol/l glucose. As shown in Figure 7, K_{ATP} channel opener diazoxide (200 μ M) evoked remarkable hyperpolarization (-77 ± 5 mV), application of ZD7288 (50 μ M) caused further hyperpolarization (-84 ± 4 mV) which could be reversed by K_{ATP} channel blocker, tolbutamide (300 μ M). In average, ZD7288 caused 17% increased hyperpolarization compared to the membrane potential change induced by diazoxide (Fig. 7B).

Influence of I_h on insulin secretion in extracellular solution containing 2.5 mmol/l KCl

Using islet perfusion, we examined biphasic glucose-stimulated insulin secretion in islets at low potassium conditions. At 2.8 mmol/l glucose, no difference was observed between HCN2-AYA and GFP groups (3.6 ± 0.5 vs. 3.7 ± 0.2 , Fig. 8) as quantified by area under the curve (AUC) analysis. At 16.7 mmol/l glucose, islets treated with HCN2-AYA displayed a similar level of insulin secretion in the first phase, and a markedly lower level in the second phase compared with GFP control (52.6 ± 1.9 vs. 63.7 ± 3.2 , Fig. 8).

DISCUSSION

We have recently demonstrated the presence of HCN channels in mouse and rat pancreatic β -cells (El Kholy *et al.* 2007), whereas their functions are still unclear. We and others found that the HCN channel antagonist, ZD7288, has a I_h -independent inhibitory effect on exocytosis, and the three other HCN channel antagonists, cesium, cilobradine, zatebradine lead to suppression of K_v channels (Gonzalez-Iglesias *et al.* 2006; Paolisso *et al.* 1985; Satoh & Yamada 2002; El Kholy *et al.* 2007). These I_h -independent effects hampered use of these reagents in some functional studies. To circumvent these problems, in the present study, we investigated the functional characterization of HCN channels by manipulating HCN channel expression genetically in primary β -cells.

Our voltage-clamp data clearly show that over-expression of HCN2 can effectively enhance I_h , and over-expression of HCN2-AYA almost completely suppresses I_h . It has been proposed that different HCN isoforms could co-assemble to form heteromers of HCN channels (Chen *et al.* 2001; Whitaker *et al.* 2007). Some evidence from studies using dominant-negative strategies has confirmed this notion. For example, in the neonatal ventricle, HCN2-AYA almost completely suppressed the native current mainly encoded by HCN2 and HCN4 in a dominant-negative manner (Er *et al.* 2003). It is also reported that a dominant-negative HCN2 pore mutant was able to suppress both HCN2 and HCN1 wild-type channels (Xue *et al.* 2002). Here, the fact that HCN2-AYA almost completely blocked native I_h in rat β -cells (where four HCN isoforms are present), indicates different HCN isoforms can co-assemble to form heteromeric channel complexes in pancreatic β -cells.

In the current-clamp experiments, our results reveal that suppression of I_h significantly enhanced membrane input resistance (R_{in}), while over-expression of I_h reduced R_{in} , indicating that I_h is a regulator in determining R_{in} in pancreatic β -cells. R_{in} is an important parameter of the intrinsic membrane properties. According to Ohm's law ($V = I R_{in}$), modulation of R_{in} will adjust the response of cell membrane potential (V) to the input current stimulus (I). Thus, our

finding suggests that I_h may play a role to modulate β -cell membrane potential responses by modulating R_{in} . Of note, besides the traditional voltage- and time-dependent component of HCN current, various studies suggest there also is an instantaneous, or voltage-independent, component (I_{inst}) of HCN currents that may represent ion flow through a "leaky" channel (Proenza *et al.* 2002; Proenza & Yellen 2006). Therefore, both of the two components may contribute to the effect of HCN channels on R_{in} , and this may explain the observation that there were differences in input resistance between groups during injection of -20 pA current (Fig 5B), where the corresponding voltage is positive to the threshold for activation of the time-dependent component of HCN currents (around -70 to -80 mV).

HCN current is reported to function as a safety inward current that helps prevent the membrane from hyperpolarization so that the cell membrane potential is maintained at appropriate levels (Williams *et al.* 2002). However, our data show that suppression of I_h did not significantly affect membrane potential at either low or high glucose in standard extracellular solution containing 5.6 mmol/l KCl (Fig. 6), indicating the native I_h may not be sufficient to influence the islet cell membrane potential at the conditions tested. We then examined the effect of I_h on membrane hyperpolarization in a low potassium extracellular solution ($[K^+]_o$), because theoretically, decrease of the $[K^+]_o$ could shift the cell resting potential to a more hyperpolarized voltage, where HCN channels are in a more activated state. Indeed, under low $[K^+]_o$ conditions, blockade of I_h by ZD7288 induced an increased membrane hyperpolarization. The effect of ZD7288 on membrane potential was unlikely due to effects on other channels, because we find that ZD7288 has no effects on voltage-dependent potassium channels, calcium channels and K_{ATP} channels (El Kholy 2007). The results therefore indicate that I_h in β -cells possess the potential to counteract membrane over-hyperpolarization at least under low $[K^+]_o$ conditions.

Our previous report suggests that knock-down of HCN channel protein by siRNA does not influence insulin secretion under normal K^+ conditions in insulinoma MIN6 cells (El Kholy *et al.* 2007). In the present study, we have verified the results by dominant-negative suppression of HCN channels using HCN2-AYA in rat islets. Our data demonstrate suppression of I_h did not affect insulin secretion and application of forskolin/IBMX to increase intracellular cAMP could not change the influence of I_h on insulin secretion at standard extracellular K^+ concentrations (Fig 4), suggesting I_h is not sufficient to modulate insulin release under normal $[K^+]_o$ conditions.

Under low $[K^+]_o$ conditions, however, a higher level of insulin secretion (especially for the second phase) was observed in control group at 16.7 mmol/l glucose but not at 2.8 mmol/l glucose in comparison with HCN2-AYA (Fig 8), suggesting that HCN channels can facilitate glucose-induced insulin secretion under the conditions tested. This phenomenon is probably due to the activation of HCN channels rendered by the preceding low glucose, low $[K^+]_o$ conditions (where HCN channels in β -cells are in a more activated state compared with normal $[K^+]_o$ conditions), because studies have revealed that activation of HCN channels can also lead to enhancement of subsequent stimulus-induced synaptic transmission in dorsal root ganglion neurons (Yu *et al.* 2004) and crayfish (Beaumont & Zucker 2000; Beaumont *et al.* 2002). The mechanism of HCN channel modulation of exocytosis remains to be elucidated, but two possibilities have been raised: (1) fractional Ca^{2+} influx and accumulation through HCN channels (Yu *et al.* 2004), (2) the involvement of actin cytoskeleton in the interaction between HCN channels and exocytotic machinery (Beaumont & Zucker 2000; Beaumont *et al.* 2002; Zhong & Zucker 2004). Further studies are needed to clarify the involved mechanisms. Nevertheless, in the case of I_h in β -cells, our results suggest a potential role for HCN channels in regulating insulin secretion under low $[K^+]_o$ conditions.

It is worth pointing out that hypokalemia (i.e. serum K^+ concentration < 3.6 mmol/lol/l) is thought to be the most common electrolyte abnormality encountered in clinical practice, and is found in over 20% of hospitalized patients (Gennari 1998). In diabetes mellitus, hypokalemia often develops, particular in patients with diabetic ketoacidosis (Gennari 1998). Thus, it is likely that I_h in β -cells may play a protective role under these pathophysiological conditions.

Acknowledgments

The majority of this work was supported by operating grants from the Canadian Institutes of Health Research to M.B.W (MOP 49521). Other contributions: Q.W (MOP 79534) from CIHR, R.B.R (PPG HL-28958) from NIH and H.Y.G from the Juvenile Diabetes Research Foundation (1-2005-1112). Q.W was a Canadian Diabetes Association Scholar and is a recipient of a New Investigator Award from CIHR. The authors thank C. J. Mahowald and Y. C. Huang (University of Toronto, Canada) for assistance with manuscript preparation. The authors declare that there is no conflict of interest that would prejudice the impartiality of this scientific work.

Reference List

- Accili EA, Proenza C, Baruscotti M, DiFrancesco D. From funny current to HCN channels: 20 years of excitation. *News in physiological sciences* 2002;17:32–37. [PubMed: 11821534]
- Beaumont V, Zhong N, Froemke RC, Ball RW, Zucker RS. Temporal synaptic tagging by $I(h)$ activation and actin: involvement in long-term facilitation and cAMP-induced synaptic enhancement. *Neuron* 2002;33:601–613. [PubMed: 11856533]
- Beaumont V, Zucker RS. Enhancement of synaptic transmission by cyclic AMP modulation of presynaptic I_h channels. *Nature neuroscience* 2000;3:133–141.
- Chen S, Wang J, Siegelbaum SA. Properties of hyperpolarization-activated pacemaker current defined by coassembly of HCN1 and HCN2 subunits and basal modulation by cyclic nucleotide. *The Journal of general physiology* 2001;117:491–504. [PubMed: 11331358]
- Dai FF, Zhang Y, Kang Y, Wang Q, Gaisano HY, Braunewell KH, Chan CB, Wheeler MB. The neuronal Ca^{2+} sensor protein visinin-like protein-1 is expressed in pancreatic islets and regulates insulin secretion. *The Journal of biological chemistry* 2006;281:21942–21953. [PubMed: 16731532]
- DiFrancesco D. Pacemaker mechanisms in cardiac tissue. *Annual review of physiology* 1993;55:455–472.
- El Kholy, W. University of Toronto; 2007. The role of hyperpolarization activated cyclic nucleotide modulated and voltage gated potassium channels in pancreatic beta-cell function.
- El Kholy W, MacDonald PE, Fox JM, Bhattacharjee A, Xue T, Gao X, Zhang Y, Stieber J, Li RA, Tsushima RG, Wheeler MB. Hyperpolarization-activated cyclic nucleotide-gated channels in pancreatic beta-cells. *Molecular endocrinology* 2007;21:753–764. [PubMed: 17158221]
- Er F, Larbig R, Ludwig A, Biel M, Hofmann F, Beuckelmann DJ, Hoppe UC. Dominant-negative suppression of HCN channels markedly reduces the native pacemaker current $I(f)$ and undermines spontaneous beating of neonatal cardiomyocytes. *Circulation* 2003;107:485–489. [PubMed: 12551875]
- Gennari FJ. Hypokalemia. *The New England journal of medicine* 1998;339:451–458. [PubMed: 9700180]
- Gonzalez-Iglesias AE, Kretschmannova K, Tomic M, Stojilkovic SS. ZD7288 inhibits exocytosis in an HCN-independent manner and downstream of voltage-gated calcium influx in pituitary lactotrophs. *Biochemical and biophysical research communications* 2006;346:845–850. [PubMed: 16780797]
- Kaupp UB, Seifert R. Molecular diversity of pacemaker ion channels. *Annual review of physiology* 2001;63:235–257.
- Koizumi A, Jakobs TC, Masland RH. Inward rectifying currents stabilize the membrane potential in dendrites of mouse amacrine cells: patch-clamp recordings and single-cell RT-PCR. *Molecular vision* 2004;10:328–340. [PubMed: 15152185]
- Ludwig A, Zong X, Jeglitsch M, Hofmann F, Biel M. A family of hyperpolarization-activated mammalian cation channels. *Nature* 1998;393:587–591. [PubMed: 9634236]

- Ludwig A, Zong X, Stieber J, Hullin R, Hofmann F, Biel M. Two pacemaker channels from human heart with profoundly different activation kinetics. *The EMBO journal* 1999;18:2323–2329. [PubMed: 10228147]
- MacDonald PE, Ha XF, Wang J, Smukler SR, Sun AM, Gaisano HY, Salapatek AM, Backx PH, Wheeler MB. Members of the Kv1 and Kv2 voltage-dependent K(+) channel families regulate insulin secretion. *Molecular endocrinology* 2001;15:1423–1435. [PubMed: 11463864]
- MacDonald PE, Sewing S, Wang J, Joseph JW, Smukler SR, Sakellaropoulos G, Wang J, Saleh MC, Chan CB, Tsushima RG, Salapatek AM, Wheeler MB. Inhibition of Kv2.1 voltage-dependent K+ channels in pancreatic beta-cells enhances glucose-dependent insulin secretion. *The Journal of biological chemistry* 2002;277:44938–44945. [PubMed: 12270920]
- MacDonald PE, Wheeler MB. Voltage-dependent K(+) channels in pancreatic beta cells: role, regulation and potential as therapeutic targets. *Diabetologia* 2003;46:1046–1062. [PubMed: 12830383]
- Magee JC. Dendritic hyperpolarization-activated currents modify the integrative properties of hippocampal CA1 pyramidal neurons. *The Journal of neuroscience* 1998;18:7613–7624. [PubMed: 9742133]
- Manning Fox JE, Gyulhandanyan AV, Satin LS, Wheeler MB. Oscillatory membrane potential response to glucose in islet beta-cells: a comparison of islet-cell electrical activity in mouse and rat. *Endocrinology* 2006;147:4655–4663. [PubMed: 16857746]
- Meuth SG, Kanyshkova T, Meuth P, Landgraf P, Munsch T, Ludwig A, Hofmann F, Pape HC, Budde T. Membrane resting potential of thalamocortical relay neurons is shaped by the interaction among TASK3 and HCN2 channels. *Journal of neurophysiology* 2006;96:1517–1529. [PubMed: 16760342]
- Paolisso G, Nenquin M, Meissner HP, Henquin JC. The effects of cesium chloride on insulin release, ionic fluxes and membrane potential in pancreatic B-cells. *Biochimica et biophysica acta* 1985;844:200–208. [PubMed: 3882155]
- Pape HC. Queer current and pacemaker: the hyperpolarization-activated cation current in neurons. *Annual review of physiology* 1996;58:299–327.
- Poolos NP, Bullis JB, Roth MK. Modulation of h-channels in hippocampal pyramidal neurons by p38 mitogen-activated protein kinase. *The Journal of neuroscience* 2006;26:7995–8003. [PubMed: 16870744]
- Poolos NP, Migliore M, Johnston D. Pharmacological upregulation of h-channels reduces the excitability of pyramidal neuron dendrites. *Nature neuroscience* 2002;5:767–774.
- Proenza C, Angoli D, Agranovich E, Macri V, Accili EA. Pacemaker channels produce an instantaneous current. *The Journal of biological chemistry* 2002;277:5101–5109. [PubMed: 11741901]
- Proenza C, Yellen G. Distinct populations of HCN pacemaker channels produce voltage-dependent and voltage-independent currents. *The Journal of general physiology* 2006;127:183–190. [PubMed: 16446506]
- Qu J, Barbuti A, Protas L, Santoro B, Cohen IS, Robinson RB. HCN2 overexpression in newborn and adult ventricular myocytes: distinct effects on gating and excitability. *Circulation research* 2001;89:E8–E14. [PubMed: 11440985]
- Robinson RB, Siegelbaum SA. Hyperpolarization-activated cation currents: from molecules to physiological function. *Annual review of physiology* 2003;65:453–480.
- Rorsman P, Bokvist K, Ammala C, Eliasson L, Renstrom E, Gabel J. Ion channels, electrical activity and insulin secretion. *Diabète & métabolisme* 1994;20:138–145.
- Santoro B, Grant SG, Bartsch D, Kandel ER. Interactive cloning with the SH3 domain of N-src identifies a new brain specific ion channel protein, with homology to eag and cyclic nucleotide-gated channels. *Proceedings of the National Academy of Sciences of the United States of America* 1997;94:14815–14820. [PubMed: 9405696]
- Santoro B, Liu DT, Yao H, Bartsch D, Kandel ER, Siegelbaum SA, Tibbs GR. Identification of a gene encoding a hyperpolarization-activated pacemaker channel of brain. *Cell* 1998;93:717–729. [PubMed: 9630217]
- Satoh TO, Yamada M. Multiple inhibitory effects of zatebradine (UL-FS 49) on the electrophysiological properties of retinal rod photoreceptors. *Pflügers Archiv: European journal of physiology* 2002;443:532–540.

- Targonsky ED, Dai F, Koshkin V, Karaman GT, Gyulkhandanyan AV, Zhang Y, Chan CB, Wheeler MB. alpha-lipoic acid regulates AMP-activated protein kinase and inhibits insulin secretion from beta cells. *Diabetologia* 2006;49:1587–1598. [PubMed: 16752177]
- Tian L, Shipston MJ. Characterization of hyperpolarization-activated cation currents in mouse anterior pituitary, AtT20 D16:16 corticotropes. *Endocrinology* 2000;141:2930–2937. [PubMed: 10919281]
- Wahl-Schott C, Biel M. HCN channels: Structure, cellular regulation and physiological function. *Cellular and molecular life sciences*. 2008
- Wendt A, Birnir B, Buschard K, Gromada J, Salehi A, Sewing S, Rorsman P, Braun M. Glucose inhibition of glucagon secretion from rat alpha-cells is mediated by GABA released from neighboring beta-cells. *Diabetes* 2004;53:1038–1045. [PubMed: 15047619]
- Whitaker GM, Angoli D, Nazzari H, Shigemoto R, Accili EA. HCN2 and HCN4 isoforms self-assemble and co-assemble with equal preference to form functional pacemaker channels. *The Journal of biological chemistry* 2007;282:22900–22909. [PubMed: 17553794]
- Williams SR, Christensen SR, Stuart GJ, Hausser M. Membrane potential bistability is controlled by the hyperpolarization-activated current I(H) in rat cerebellar Purkinje neurons in vitro. *The Journal of physiology* 2002;539:469–483. [PubMed: 11882679]
- Xiao J, Nguyen TV, Ngui K, Strijbos PJ, Selmer IS, Neylon CB, Furness JB. Molecular and functional analysis of hyperpolarisation-activated nucleotide-gated (HCN) channels in the enteric nervous system. *Neuroscience* 2004;129:603–614. [PubMed: 15541882]
- Xue T, Marban E, Li RA. Dominant-negative suppression of. *Circulation research* 2002;90:1267–1273. [PubMed: 12089064]
- Yagi J, Sumino R. Inhibition of a hyperpolarization-activated current by clonidine in rat dorsal root ganglion neurons. *Journal of neurophysiology* 1998;80:1094–1104. [PubMed: 9744924]
- Yu X, Duan KL, Shang CF, Yu HG, Zhou Z. Calcium influx through hyperpolarization-activated cation channels (I(h) channels) contributes to activity-evoked neuronal secretion. *Proceedings of the National Academy of Sciences of the United States of America* 2004;101:1051–1056. [PubMed: 14724293]
- Zhang Y, Zhang N, Gyulkhandanyan AV, Xu E, Gaisano HY, Wheeler MB, Wang Q. Presence of functional hyperpolarisation-activated cyclic nucleotide-gated channels in clonal alpha cell lines and rat islet alpha cells. *Diabetologia* 2008;51:2290–2298. [PubMed: 18850083]
- Zhong N, Zucker RS. Roles of Ca²⁺, hyperpolarization and cyclic nucleotide-activated channel activation, and actin in temporal synaptic tagging. *The Journal of neuroscience* 2004;24:4205–4212. [PubMed: 15115816]

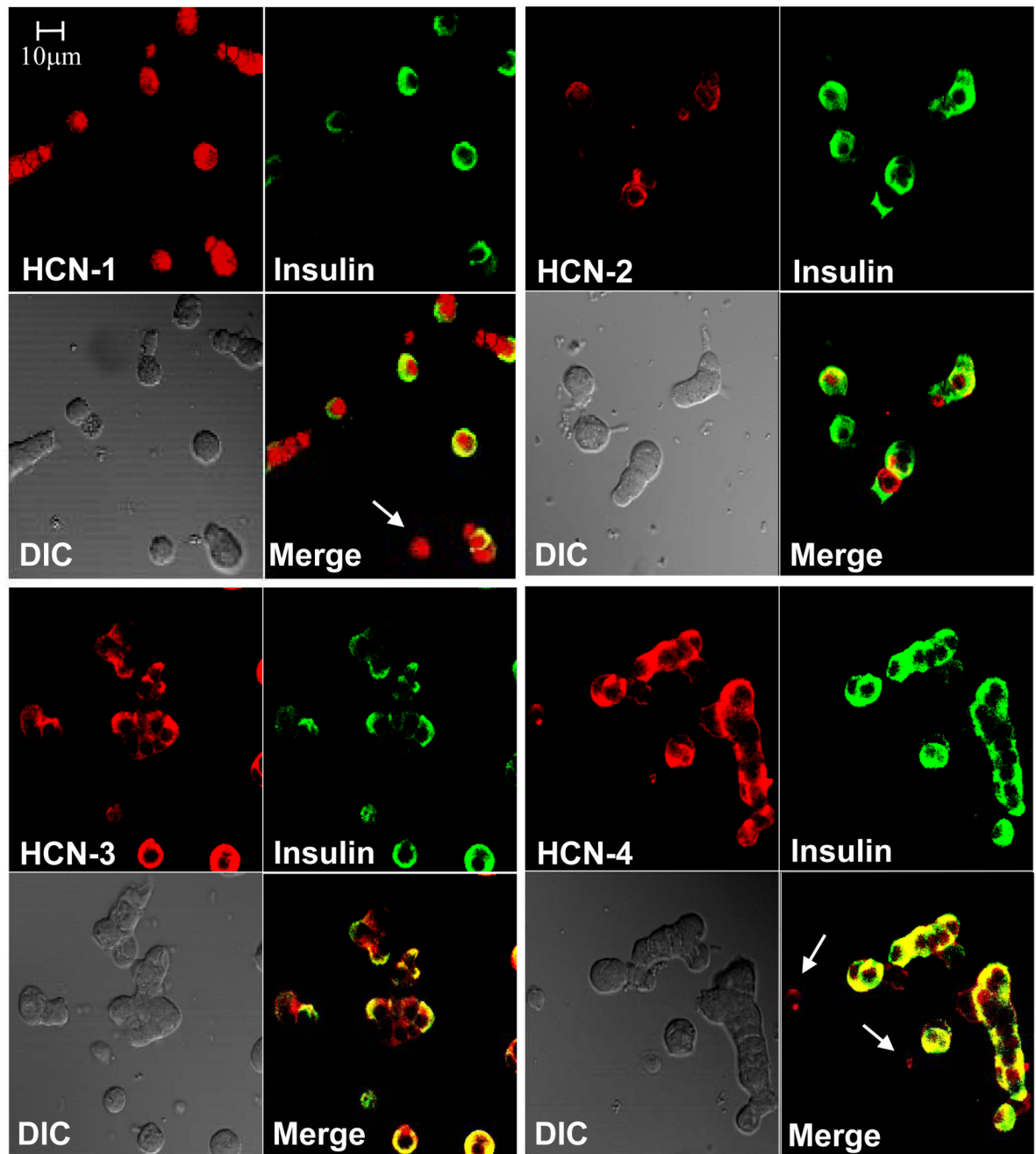


Figure 1. Expression of HCN proteins in pancreatic rat islet cells

Representative confocal laser scanning microscopy images of dispersed rat islet cells which were dual-stained for each of the HCN isoforms (red) and insulin (green). Light (left) and merged images (right) are shown in the lower panels of each group.

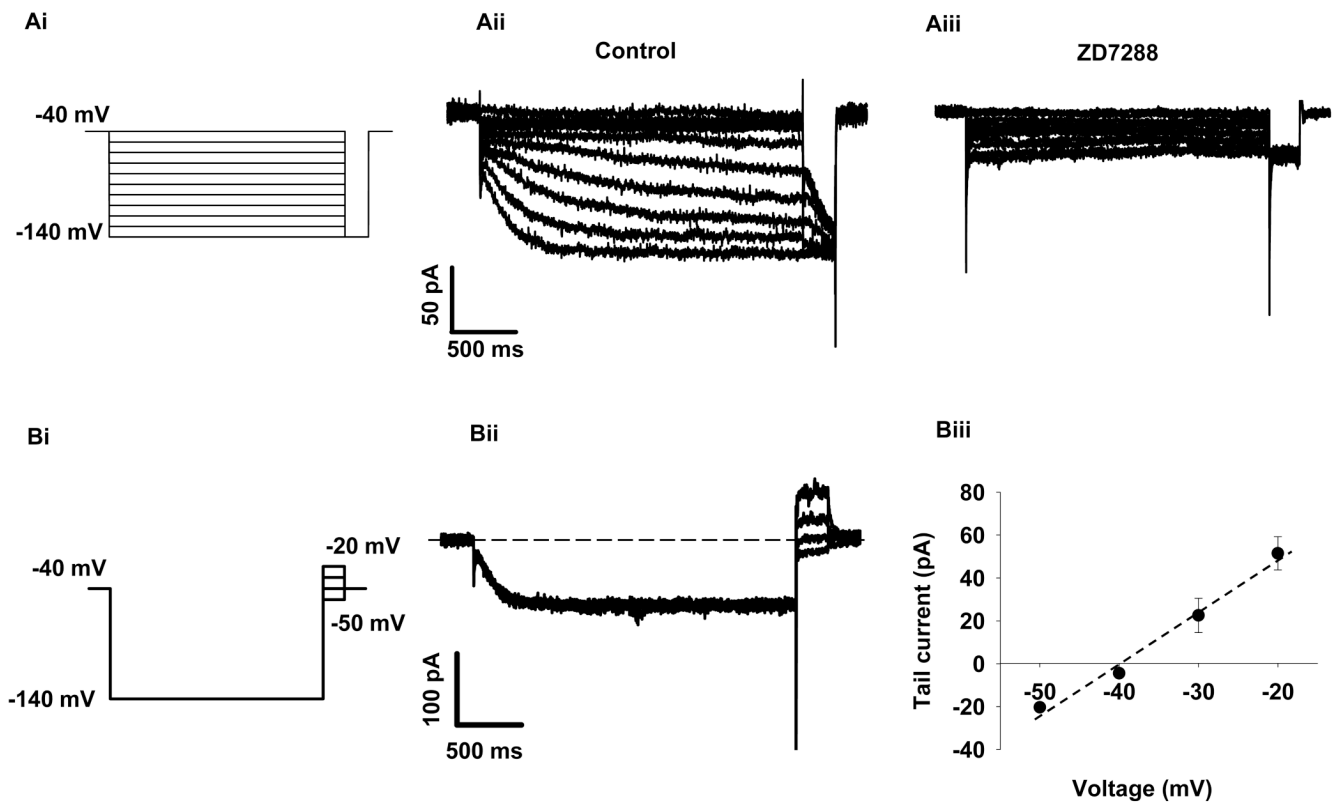


Figure 2. Characteristics of native I_h in rat β -cells

A, Effect of ZD7288 on I_h . Cells were clamped from a holding potential of -40 mV to various voltages (-140 to -40 mV) for 2.5 seconds followed by a step to -140 mV (Ai). The slow hyperpolarization-activated I_h currents were induced with this voltage protocol under control conditions (Aii); and ZD7288 (50 μ M), an I_h inhibitor, blocked $67.9 \pm 7.2\%$ of I_h at -140 mV ($p < 0.01$, $n = 6$, Aiii). B, Determination of current-voltage relationship of the fully activated HCN channels. To obtain the I/V relationship, a family of 250 ms test pulses ranging from -70 mV to -20 mV were applied to β -cells after a 2.5 -second pre-pulse to -140 mV (Bi, voltage protocol). Bii showed the typical series of current traces, the dashed line indicates zero current. The I/V curve was made by plotting tail currents against test potentials (right panel, $n = 6$) showing the reversal potential is -38 mV (Biii). Data shown are mean \pm SEM.

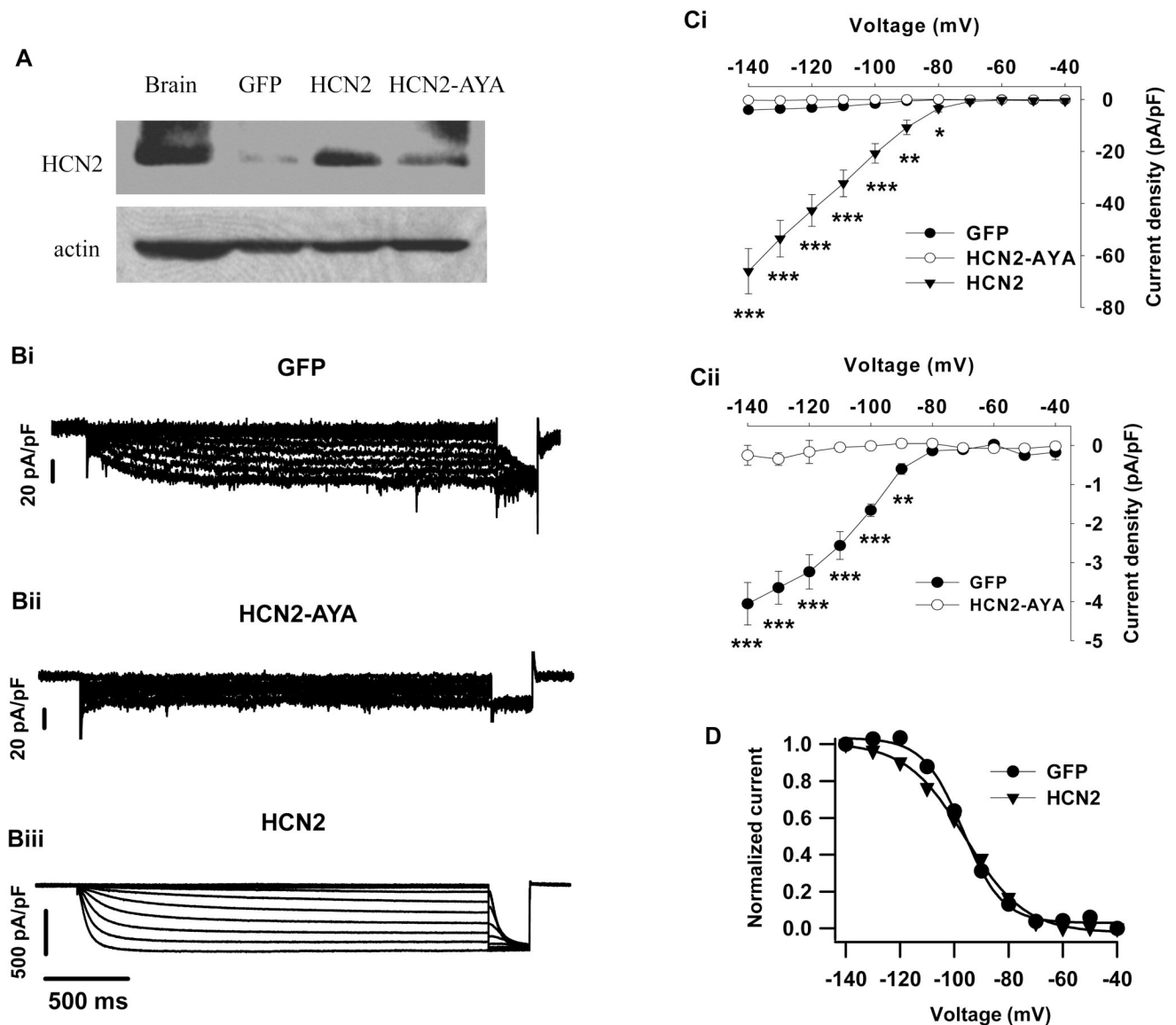


Figure 3. Effects of up-regulation and dominant-negative suppression of HCN channels on I_h in rat β -cells

A. Western blotting showing the effect of HCN2 or HCN2-AYA infection on HCN2 protein levels in rat islet cells. Rat brain was used as positive control. β -actin was examined to assess the protein loading of the lanes. B. Representative current traces of I_h were recorded in GFP (Bi), HCN2-AYA (Bii) and HCN2-transduced cells (Biii). Different vertical scales were indicated. Voltage protocol was identical in figure 2A and figure 3B. Ci, Steady-state current-voltage relationships were obtained by plotting the sustained inward currents with corresponding test voltages. Cii was the expanded vertical scale of Bi to clearly show the effect of HCN2-AYA on I_h compared to control. D. Steady-state voltage activation curves of I_h in GFP and HCN2-transduced cells. The tail currents measured immediately after the voltage step to -140 mV were normalized and fit by the Boltzmann function. The membrane potentials of half-maximal activation ($V_{1/2}$) were obtained as -97 ± 1 mV in GFP control ($n=6$) and -96 ± 1 mV in HCN2 ($n=6$), respectively. Data shown are mean \pm SEM, * $p < 0.05$, ** $p < 0.01$ and *** $p < 0.001$, respectively, compared with the control.

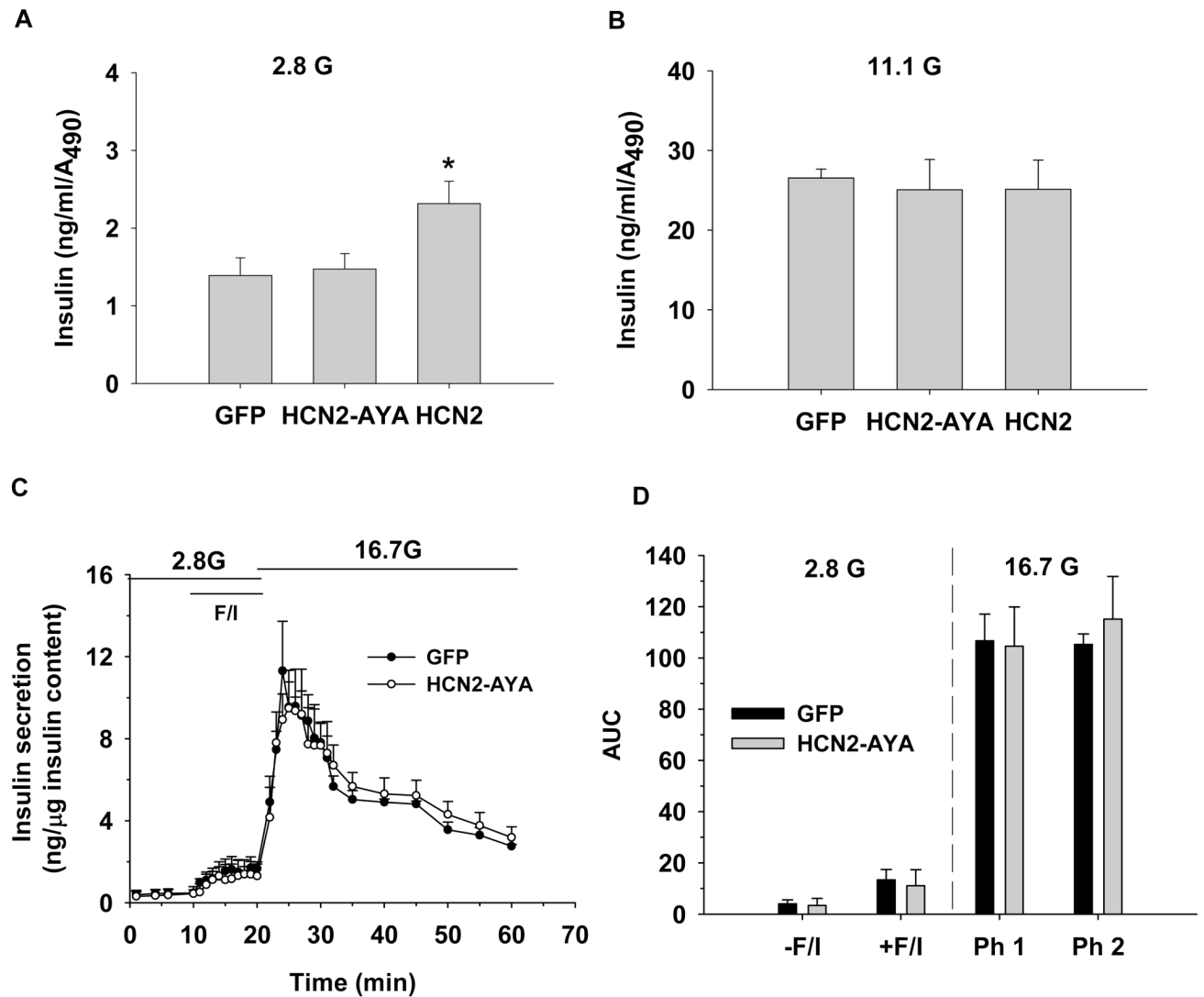


Figure 4. Influence of I_h on insulin secretion

A–B. The islet static insulin secretion assay was performed and the amount of insulin were measured at 2.8 mmol/l glucose (2.8 G) and 11.1 mmol/l glucose (11.1 G), data were then normalized to the absorbance from XTT assay (n=5). C. The islet perfusion insulin secretion assay was performed and the amount of insulin were measured at 2.8 mmol/l glucose (2.8 G) and 16.7 mmol/l glucose (16.7 G) in the presence or absence of forskolin (10 μM) plus IBMX (100 μM), F/I indicate forskolin plus IBMX. Insulin released was normalized to total insulin content. D. Average of area under curves (AUC) of insulin levels during islet perfusion from C (n=4). The first phase (Ph1) of insulin secretion at 16.7 mmol/l glucose was quantified from 20–35 min and the second phase (Ph2) from 35–60 min from C. Data shown are mean ± SEM, * p < 0.05 compared with GFP control

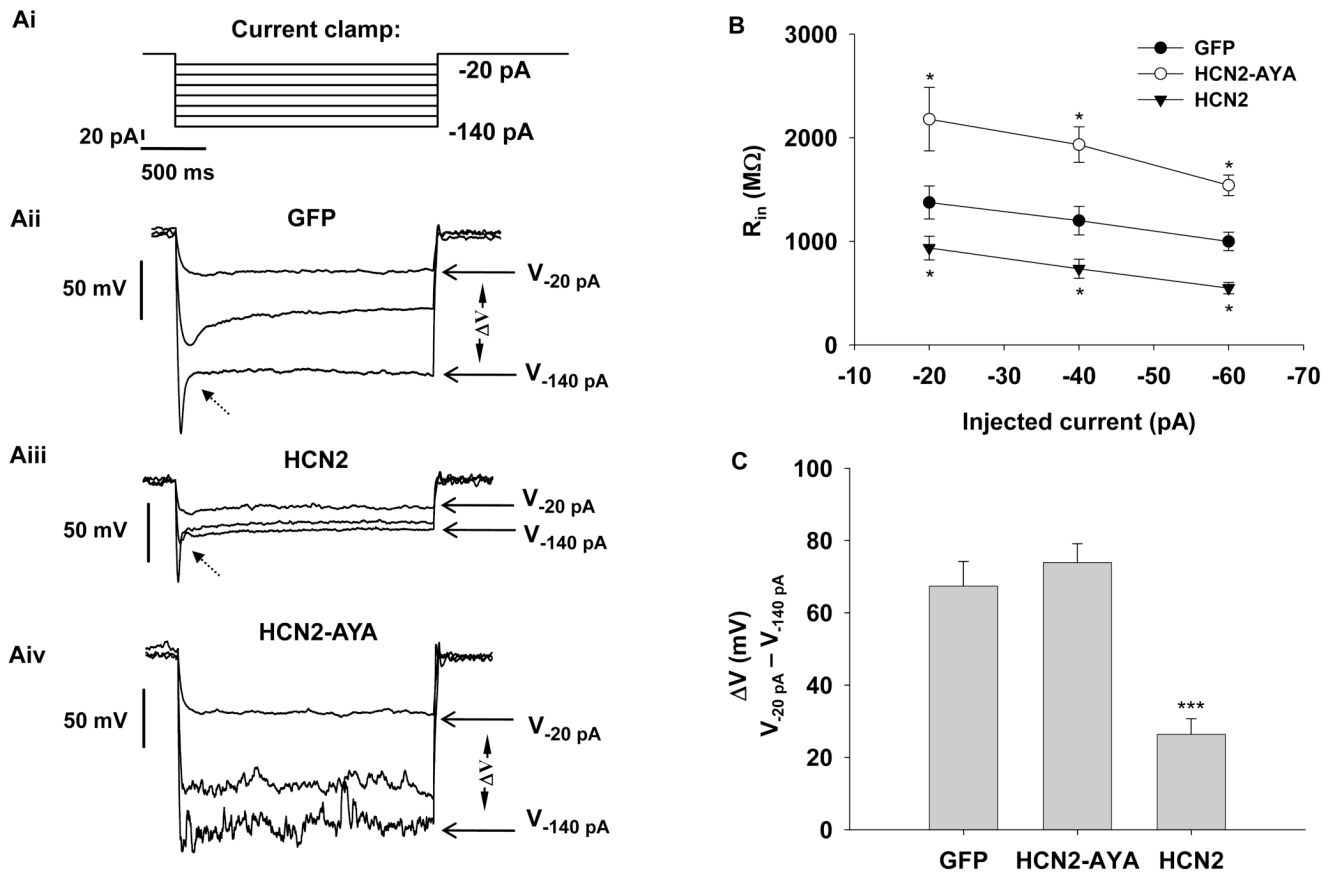


Figure 5. Influence of I_h on input resistance (R_{in})

Ai, Stimulus protocol under current-clamp mode, resting potential was held at -40 mV by injecting constant current. The voltage responses were induced by additional hyperpolarizing currents ranging from -20 pA to -140 pA with a 20 pA increment. Representative current-clamp recordings in response to injected hyperpolarizing currents in rat β -cells transduced with GFP (Aii), HCN2 (Aiii) or HCN2-AYA (Aiv) are shown. For clarity, only voltages induced by -20 , -60 and -140 pA injected currents are included. The dashed arrow indicated depolarizing “sag”. B, Summary of input resistance obtained by the average of the voltage responded to a set of injected hyperpolarizing currents. C, Group data for the difference between the two voltages in response to -20 pA and -140 pA of injected currents ($\Delta V = V_{-20 \text{ pA}} - V_{-140 \text{ pA}}$) showing the stabilizing effect of I_h on membrane potential. Data shown are means \pm SEM, * $p < 0.05$ and *** $p < 0.001$, respectively, compared with the control.

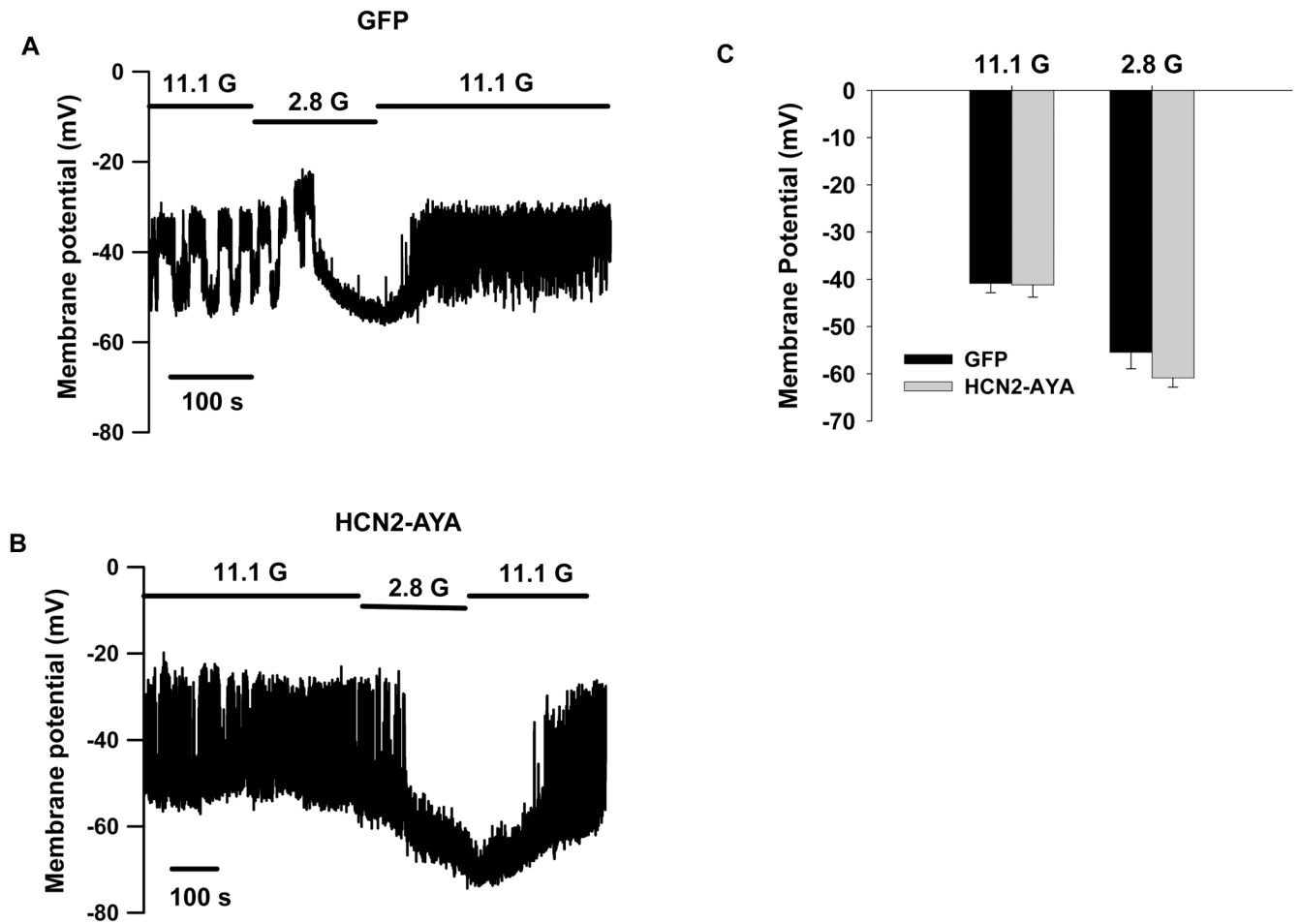


Figure 6. Influence of I_h on membrane potential in standard extracellular solution containing 5.6 mmol/l KCl

Membrane potentials were recorded without current injection in rat islet β -cells transduced with GFP (A) or HCN2-AYA (B) in the presence of 11.1 mmol/l (11.1 G) and 2.8 mmol/l (2.8 G) glucose. C, Summary of mean membrane potentials at 11.1 and 2.8 mmol/l glucose (n=5 for each).

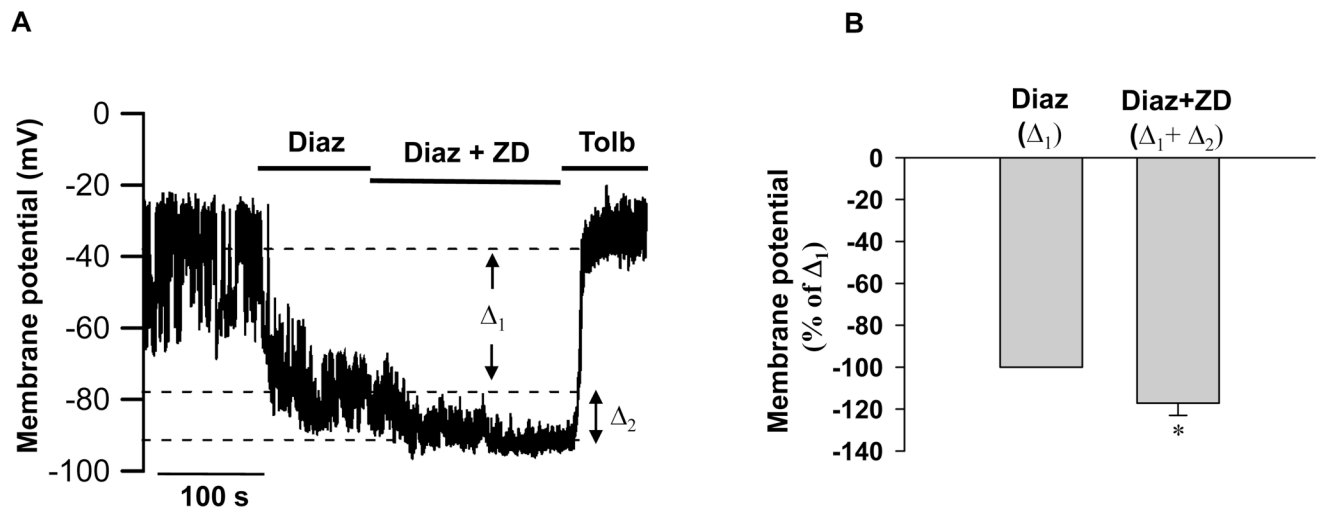


Figure 7. Influence of I_h on membrane hyperpolarization in extracellular solution containing 2.5 mmol/l KCl

Membrane potentials were recorded without current injection. A, Rat islet β -cells were perfused with solution containing 11.1 mmol/l glucose and were then challenged with 200 μ M diazoxide (Diaz) in the absence or presence of 50 μ M ZD7288 (ZD) followed by perfusion of 300 μ M Tolbutamide (Tolb). B, Bar graph shows the normalized changes of mean membrane potentials (to Δ_1 induced by Diazoxide), Δ_2 is the excessive change induced by ZD7288 at the presence of diazoxide (n=6). Data shown are mean \pm SEM, * $p < 0.05$ by paired t test.

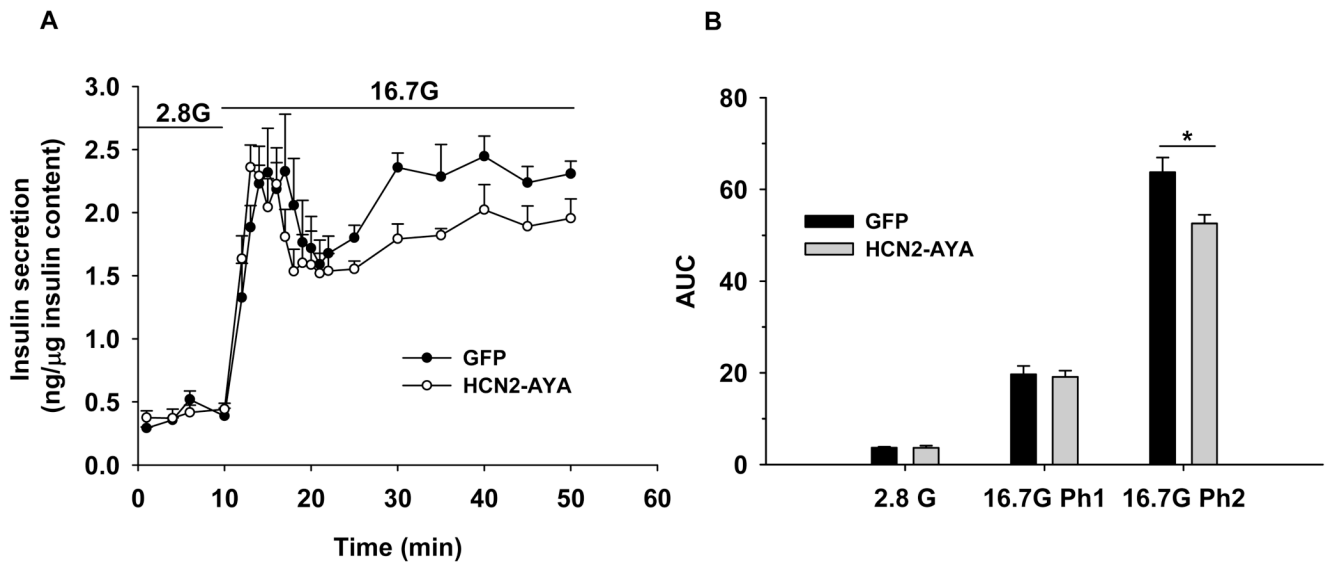


Figure 8. Influence of I_h on insulin secretion in extracellular solution containing 2.5 mmol/l KCl
 A. Islet perfusion insulin secretion assay was performed and the amount of insulin were measured at 2.8 mmol/l glucose (2.8 G) and 16.7 mmol/l glucose (16.7 G) as indicated, insulin released was normalized to total insulin content. B. Average of area under curves (AUC) of insulin levels during islet perfusion from A (n=4). The first phase (Ph1) of insulin secretion at 16.7 mmol/l glucose was quantified from 10–21 min and the second phase (Ph2) from 21–50 min from A. Data shown are mean \pm SEM, * $p < 0.05$ compared with GFP control.